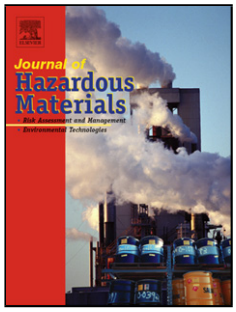

Title: Characterization and improved solar light activity of vanadium doped TiO_2/diatomite hybrid catalysts

Author: Bin Wang Guangxin Zhang Xue Leng Zhiming Sun Shuilin Zheng

PII: S0304-3894(14)00938-8
DOI: http://dx.doi.org/doi:10.1016/j.jhazmat.2014.11.031
Reference: HAZMAT 16403

To appear in: *Journal of Hazardous Materials*

Received date: 12-8-2014
Revised date: 17-11-2014
Accepted date: 21-11-2014

Please cite this article as: Bin Wang, Guangxin Zhang, Xue Leng, Zhiming Sun, Shuilin Zheng, Characterization and improved solar light activity of vanadium doped TiO2/diatomite hybrid catalysts, Journal of Hazardous Materials http://dx.doi.org/10.1016/j.jhazmat.2014.11.031

Characterization and improved solar light activity of vanadium doped TiO_2/diatomite hybrid catalysts

Bin Wang[a,b] b.wang6@uq.edu.au, Guangxin Zhang[a] z111@163.com, Xue Leng[b] xue.leng@uq.net.au, Zhiming Sun[a] zhiming.baxia@163.com, Shuilin Zheng[a*] shuilinzheng8@gmail.com

[a] School of Chemical and Environmental Engineering, China University of Mining & Technology, Beijing 100083, PR China

[b] School of Chemistry and Molecular Biosciences, The University of Queensland, Brisbane Qld 4072, Australia

Fax: +86 10 62390972.

Graphical Abstract

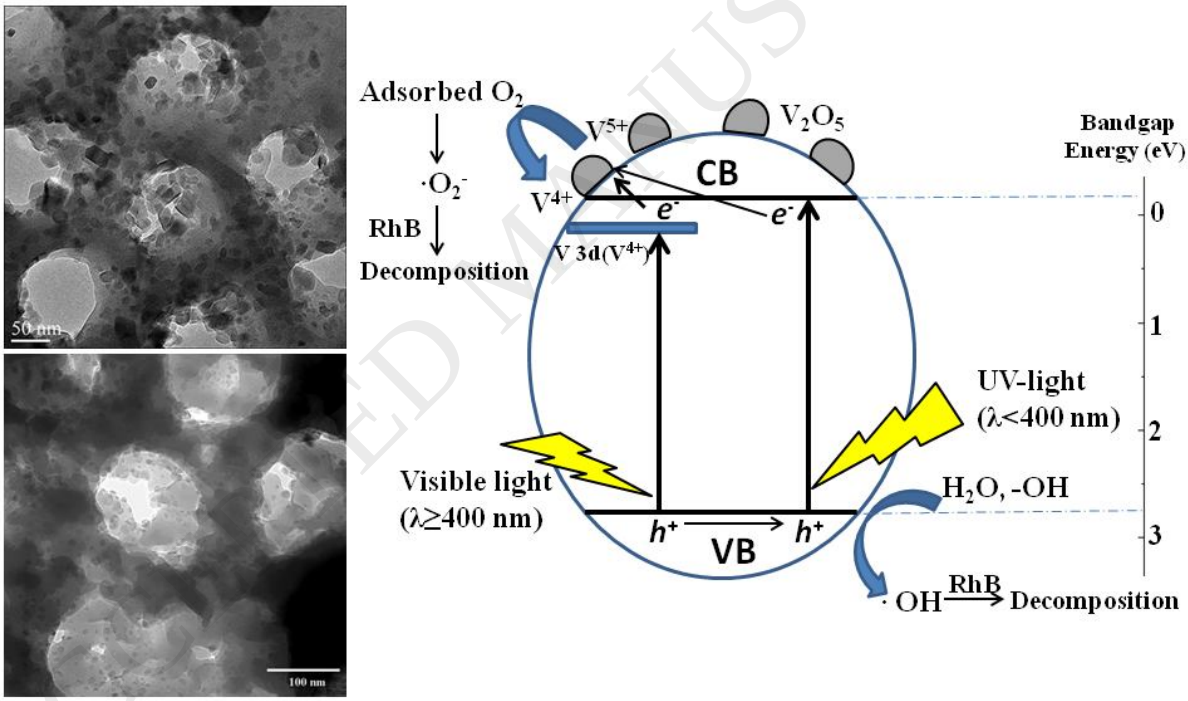

Highlights

- V-doped TiO_2/diatomite composite photocatalyst was synthesized.
- The physiochemical property and solar light photoactivity were characterized.
- The presence and influence of V ions in TiO_2 matrix was systematically analyzed.

- The photocatalysis for Rhodamine B were studied under solar light illumination.

Abstract

V-doped TiO_2/diatomite composite photocatalysts with different vanadium concentrations were synthesized by a modified sol–gel method. The diatomite was responsible for the well dispersion of TiO_2 nanoparticles on the matrix and consequently inhibited the agglomeration. V-TiO_2/diatomite hybrids showed red shift in TiO_2 absorption edge with enhanced absorption intensity. Most importantly, the dopant energy levels were formed in the TiO_2 bandgap due to V^{4+} ions substituted to Ti^{4+} sites. The 0.5% V-TiO_2/diatomite photocatalyst displayed narrower bandgap (2.95 eV) compared to undoped sample (3.13 eV) and other doped samples (3.05 eV) with higher doping concentration. The photocatalytic activities of V doped TiO_2/diatomite samples for the degradation of Rhodamine B under stimulated solar light illumination were significantly improved compared with the undoped sample. In our case, V^{4+} ions incorporated in TiO_2 lattice were responsible for increased visible-light absorption and electron transfer to oxygen molecules adsorbed on the surface of TiO_2 to produce superoxide radicals $\cdot O_2^-$, while V^{5+} species presented on the surface of TiO_2 particles in the form of V_2O_5 contributed to e^-–h^+ separation. In addition, due to the combination of diatomite as support, this hybrid photocatalyst could be separated from solution quickly by natural settlement and exhibited good reusability.

Key words

photocatalytic degradation, doping TiO_2, diatomite, sol–gel method

1. Introduction

Currently, organic dyes and their effluents have become one of the main sources of water pollution due to the greater demand in industry such as textile, paper, and plastic. These organic dyes are composed of certain organic compounds, which are toxic to microorganism, aquatic life and human beings, and constituting a serious concern to the ecosystem [1]. Be different from the traditional techniques such as absorption on carbon, ultrafiltration, reverse osmosis, coagulation by chemicals, etc., photocatalysis is one of the best routes for the complete mineralization of organic compounds to CO_2, water, and mineral acids. Until now, TiO_2 photocatalyst has been widely studied because of its high corrosion and photo-corrosion

resistance in aqueous media, strong oxidizing power, environmental friendliness, and easy availability [2]. However, a major drawback of pure TiO_2 is the large bandgap, which means it can only be activated by irradiation with UV-light ($\lambda \leq 387$ nm for anatase), limiting the practical efficiency for solar applications [3]. Therefore, in order to enhance its low utilization of solar energy, it is necessary to facilitate the visible-light absorption. Transition metals doped TiO_2 has shown great promise in extending the spectral response and achieving visible-light-activated photocatalysis [4]. The incorporation of transition metals in the titania crystal lattice may result in the formation of new energy levels between valence band (VB) and conduction band (CB), indicating a shift of light absorption towards the visible-light region. Vanadium doped TiO_2 seems one of the best alternatives for this object [5, 6]. The researchers attributed the enhanced photocatalytic activity of V-doped TiO_2 to the following one or several reasons: (i) the enhanced absorption in the visible-light region; (ii) the improved quantum efficiency owing to the effective e^-–h^+ pair separation; and (iii) the presence of both V^{4+} and V^{5+} species in the V-doped TiO_2 materials. Additionally, the former can contribute to the increased visible-light absorption and electron transfer, while the latter is just a potential electron acceptor and enhances e^-–h^+ separation [7-9].

The most commonly used TiO_2 morphology is that of mono-dispersed nanoparticles wherein the diameter is controlled to give benefits from the small crystallite size (high surface area, reduced bulk recombination) without the detrimental effects associated with very small particles (surface recombination, low crystallinity) [10]. However, the fabrication procedure and apply this TiO_2 nanoparticle in pollutant elimination suffer from several difficulties, such as agglomeration, separation and recovery of fine catalyst particles, which limit to exploit its best photo-efficiency [11]. In recent years, combining TiO_2 nanoparticles with carbon materials (such as carbon nanotube, graphene and graphene oxide) or magnetic materials is an effective method to overcome these disadvantages [12-15]. Graphene oxide is a chemically modified graphene with oxygen functional groups [16]. In addition, the carbon materials may improve the e^-–h^+ pair separation as well. Unfortunately, the processing technique of these carbon materials and magnetic materials is complicated and not environmental friendly. Thus from the point of economical view, many researchers have started to study the natural support materials. Porous minerals are regarded as optimal support for photocatalyst due to their high porosity, large specific surface area, high stability and abundance. Therefore, nano-TiO_2/mineral composites have been postulated as suitable alternative photocatalyst in environmental remediation [17-23]. Because there are a lot of

silicon hydroxyls and hydrogen bonds on the surface of diatomite, which can form strong forces with TiO_2 nanoparticles. Consequently it can inhibit the agglomeration of TiO_2 and protect them from being washed away in flow system. Based on these, we have synthesized the TiO_2/diatomite hybrid catalysts by sol–gel method under facile condition [20]. Advantages of such structure are their tailored morphology, unified porosity, well reusability and high mechanical strength, which result in enhanced performance in photo-induced applications, mainly in photocatalysis.

Motivated by the above successful applications and fascinating advantages our current work focuses on the preparation of vanadium doped TiO_2/diatomite hybrids. So far, though V-doped TiO_2 nanoparticles and diatomite supported TiO_2 composites have shown either efficient visible-light photocatalytic activity or improved reusability, few reports are published on vanadium doped TiO_2/diatomite junction system. We expect that vanadium doped TiO_2/diatomite material may demonstrate a new and efficient photocatalytic system with a view to practical applications. Herein, metallic vanadium doped TiO_2/diatomite composites (V-TiO_2/diatomite) with well dispersion of TiO_2 nanoparticles on the surface of diatomite were prepared by a modified sol–gel method. This good dispersion or reduced agglomeration of TiO_2 nanoparticles is expected to increase the contact opportunity between active site and reactant and facilitate the light absorption. Accordingly, the photocatalytic efficiency of the V-TiO_2/diatomite hybrids will be increased. The physicochemical properties of the resulting hybrids were characterized by X-ray diffraction (XRD), Raman spectrometer, transmission electron microscope (TEM), X-ray photoelectron spectroscopy (XPS), UV-vis diffuse reflectance spectrometer (UV-vis DRS), and fluorophotometer. Subsequently, their solar-light photocatalytic activity was evaluated by the degradation of dye Rhodamine B. And the V concentration, adsorption behaviours of dye and recycling ability were also investigated.

2. Experimental methods

2.1. Materials

The chemicals used in the present study were of analytical grade. Tetrabutyl titanate ($C_{16}H_{36}O_4Ti$, TBOT), ethanol (C_2H_5OH), hydrochloric acid (HCl), acetic acid (CH_3COOH) and ammonium metavanadate were purchased from Sigma-Aldrich Co. LLC. For synthesis the chemicals were used as received without further purification. Rhodamine B (RhB) was purchased from Beijing Reagent Co. (Beijing, China).

2.2. Preparation of V-TiO_2/diatomite hybrid catalysts

Purified diatomite (DE) was used as carrier of the vanadium doped TiO_2/diatomite (V/TD). The purification process has been described in detail elsewhere [24]. The preparation of V/TD hybrid catalysts was undertaken by a modified sol–gel method [20]. DE suspensions with different molar ratios (0.25, 0.5, 1.0 and 1.5%) of vanadium ions were prepared by dispersing 1.0 g of DE in a mixture constituted by 14.0 mL of ethanol and 1.0 mL of acetic acid, under stirring for 30 min. Afterwards 1.5 mL of TBOT were added dropwise into the DE suspension, under continuous stirring, followed by the addition of 12.0 mL of ethanol: water solution (v: v=1:1; pH=2) which led the hydrolysis of TBOT at moderate rate. The mixture was then stirred continuously for 12 h to immobilize the as-generated TiO_2 colloids on the DE surface. The final product was dried in an oven at 105^{o}C for 4 h, followed by calcination (650^{o}C for 2 h in air, heating rate of 2.5°/min). Undoped TiO_2/diatomite (TD) was prepared by a similar method as V/TD without metal salts. Pure V-TiO_2 without diatomite as reference was also synthesized, which was denoted as V/T.

2.3. V-TiO_2/diatomite hybrid catalysts characterization

The crystal phase properties of the samples were analysed with a D8 advance X-ray diffractometer (Bruker, Germany) equipped with Cu Kα radiation (λ=0.154056 nm) in the 2θ range from 10 to 80º with a scanning rate at 4º/min. The average crystallite sizes were calculated from the di□raction line width based on Scherrer's relation: $D = 0.89\lambda / \beta \cos\theta$; where λ denotes the wavelength of X-ray and β is the corrected full width at half maxima (FWHM). Raman spectra of the samples were taken on the Renishaw inVia Raman spectrometer with a 514 nm Argon laser line. Both the spectral resolution and the accuracy in the Raman shift are estimated to be ~2 cm^{-1}. The morphology of hybrid catalysts were observed with Tecnai F20 equipped with an energy dispersive X-ray (EDX) analysis. XPS spectra were recorded using an X-ray photoelectron spectrometer (Kratos Axis Ultra) which uses Al K_α (1486.6 eV) X-ray source. The curve fitting for the high resolution C1s core level peaks was done using Casa XPS software by means of least square peak fitting procedure using a Gaussian–Lorentzian function. The optical properties of the samples were characterized by UV-vis diffuse reflectance spectroscopy (DRS) using a UV-vis spectrophotometer (Cary 500, Varian Co.), in which $BaSO_4$ was used as the internal reflectance standard. The band gap value was estimated by extrapolating the linear part of the plot of $(F(R)h\nu)^{1/2}$ versus $h\nu$: $F(R)h\nu = A(h\nu - E_g)^2$, where $F(R)=(1-R)^2/2R$ stands for the

Kubelka-Munk function calculated from the reflectance spectrum; and *hv* is the photon energy expressed in eV. The photoluminescence (PL) spectra of the samples were measured with Horiba Fluorolog-3 spectrometer using the 320 nm line of Xe lamp as the excitation source.

2.4. Photocatalytic activity measurements

Rhodamine B (RhB) was used as a model pollutant to evaluate the photocatalytic activity of the as-prepared V-TiO_2/diatomite hybrid catalysts through a kinetic test. In a typical measurement, 0.05 g of V-TiO_2/diatomite catalysts was suspended in 100 mL of standard RhB aqueous solution (10 mg/L). In the centre of tube, a 500W Xe lamp (having closet spectral match to the solar spectrum) was used as the stimulate solar-light source. Prior to illumination, the suspension was stirred in the dark for 1 h to establish an adsorption/desorption equilibrium between the photocatalyst and RhB molecules. Then, the photocatalytic degradation of RhB was initiated. Photodegradation was monitored by measuring the absorbance of the solution at 562 nm using UV-vis spectrophotometer (UV-9000S, Shanghai Yuanxi) and plotting it as a function of illumination time. A comparative experiment was carried out under the same conditions using pure V-TiO_2 particles (0.05 g) as catalysts. The recycling tests were conducted on our materials. First, the hybrids were allowed to settle down naturally in the reactor tube (which takes less than 30 min), and then were washed with ethanol and distilled water (3 times). The catalysts were then dried at 105^{o}C overnight before being reused and re-suspended in a fresh RhB solution. Recycling test was subsequently performed for four times.

3. Results and discussion

3.1. XRD and Raman analysis

To investigate the crystal structure of the prepared catalysts, we employed XRD for the samples. **Fig. 1** shows the typical XRD patterns of the prepared samples. The XRD pattern of DE is in good agreement with that of the referenced amorphous opal-A, which is a characteristic of a broad diffraction peak centred at around 2θ =21.8° [20]. And there are two characteristic diffraction peaks at 2θ = 21.4° and 27.2° corresponding to quartz. The spectra for vanadium doped TiO_2/diatomite hybrids show only the presence of anatase TiO_2 with the peaks at 25.3, 37.8, 48.1, 53.9 and 62.9^{o} representing the crystal planes for (101), (004), (200), (105) and (204), respectively [25]. There is no presence of any other polymorph for TiO_2 like rutile or brookite observed in the samples. Also, we have not observed any intense diffraction

peaks related to the oxides of vanadium, indicating that either the V was successfully incorporated into the crystal lattice of anatase TiO_2 or the vanadium oxides were dispersed well on the surface of the TiO_2 particles. The XRD intensity of the anatase peaks decrease first with the relative lower doping concentration (**Fig. 1c** and **d**). Then with an increase in doping concentration, the diffraction intensity almost keeps steady and the diffraction peaks become narrower (**Fig.1e** and **f**), indicating the formation of the larger TiO_2 crystallites and the better crystalline degree, which is an important factor affecting photocatalytic efficiency [26]. It has been reported that transition metal ions as dopant incorporated into TiO_2 might arouse the crystal lattice distortion [27]. Thus, to investigate the changes that V ions might cause in the crystal structure of TiO_2, we enlarged the anatase (101) diffraction peak of the V-TiO_2/diatomite hybrids. We can see from the spectra that with the increasing V concentration the position of the anatase (101) peak gradually shifts towards the higher diffraction angle. This suggests that the V ions might successfully incorporate into the crystal lattice of anatase TiO_2 as V^{4+} and/or V^{5+} and substituted for Ti^{4+}. Compared with V^{5+} ion (0.068 nm), the ion radius of six-coordinated V^{4+} (0.072 nm) is much closer to that of Ti^{4+} (0.074 nm) [6]. This fact implies that V^{4+} ions are easier to substitute for Ti^{4+} sites and V^{5+} ions are apt to form V_2O_5 oxides localized on the TiO_2 surface [28]. Similar results have also been found by other researchers [6, 29, 30]. Additionally, subsequent XPS and UV-vis DRS analysis results further confirm this conclusion (see ***Section 3.3*** and ***3.4***). Also, the average crystalline sizes were calculated by the help of Scherrer's formula from the diffraction plane (101) of the anatase (mentioned above in ***Section 2.3***). And the results indicate that the crystalline size of TiO_2 decreases first and then increases (**Table 1**). Thus, as depicted in **Table 1**, with the increasing vanadium doping concentration the V^{4+} species implantation inhibits crystallite growth [6, 31] and the V^{5+} species (as V_2O_5 oxides) promote it.

To further confirm that the V ions as the dopants were successfully incorporated into the TiO_2/diatomite composites, Raman spectra of undoped TiO_2/diatomite and V-doped samples are shown in **Fig. 2**. The Raman spectra of all samples correspond to the anatase phase of TiO_2. Anatase TiO_2 has six Raman active modes ($A_{1g} + 2B_{1g} + 3E_g$) [32-34]. The dominant E_g peak appears at 144 cm^{-1}. The other E_g peaks as low intense peak at 196 and 638 cm^{-1}. One B_{1g} peak appears at 396 cm^{-1} and the ($A_{1g} + B_{1g}$) peak appears at 516 cm^{-1}. Raman peak at around 144 cm^{-1} in each of the samples is attributable to the Ti–O bending vibration [35]. It can be seen that the E_g peak of TiO_2 exhibits a slight blue shift with the increasing V

concentration. This result might be attributed to the distortion of crystal lattice structure and the increased Ti–O bond strength rendered by the V^{4+} and V^{5+} ions [6, 27]. Raman result clearly indicates that the anatase crystal structure of the TiO_2 is well maintained even after vanadium cations (V^{5+}/V^{4+}) doping (it is well known that Raman spectroscopy can detect even minor amount of rutile or brookite phase [36]).

3.2. Morphology analysis

The TEM micrographs of the DE, undoped TiO_2/diatomite and V-TiO_2/diatomite samples are illustrated in **Fig. 3**. As observed from the images, the diatomite as the support exhibit highly porous disk-like shape with radius of ~10 μm (**Fig. 3a**). And this structure is maintained well even after the coating of TiO_2 nanoparticles (**Fig. 3b** and **d**). Moreover, most of TiO_2 nanoparticles exhibit irregular spherical shapes with low level of agglomeration. This indicates the intimate interaction between bare TiO_2 nanoparticles and diatom appears in this hybrid catalyst. The EDX measurement confirms the composition of the hybrids (***Inset***) and demonstrates the presence of Si, Ti and O; meanwhile Cu signal is derived from the cooper grid for TEM measurement. HRTEM image (**Fig. 3c**) of individual particles clearly shows the presence of lattice fringes hence indicating the crystalline nature of the photocatalyst particle at nano-scales. The interplanar spacing was measured to be around 0.354 nm which is in good agreement with the (101) family of planes for the anatase phase (0.352 nm) [36].

3.3 XPS analysis

The chemical states of the dopants incorporated into TiO_2 were investigated by XPS. The survey and the core levels of Ti2p, O1s, and V2p in V-TiO_2/diatomite composites are reported in **Fig.4**. **Fig. 4a** depicts the survey spectra of the prepared hybrids with different vanadium doping concentrations. The signals of Ti, O, and Si elements can be clearly observed in all the samples. In **Fig. 4b**, the two peaks centred at 458.6 and 464.3 eV are assigned to the $Ti2p_{3/2}$ and $Ti2p_{1/2}$ of TiO_2, respectively, correspond to +4 valence state of Ti [37]. The doublet peaks are due to the spin-orbit splitting of Ti2p and separated by 5.7 eV. This result suggests that TiO_2 in the product is only anatase phase, which is consistent with the XRD and Raman spectra. The Ti2p peak position is shifted by ~0.3 eV towards positive binding energy value as compared to the undoped sample (458.5 eV), thus indicating that part of V ions are incorporated into TiO_2 lattice and influence the local chemical state of Ti^{4+} ions

[36, 38]. The deconvolution of the O1s spectrum of 1.0%-V/TD shows three peaks (**Fig. 4c**), including a dominant peak at about 533.1 eV and two lower energy peaks at approximately 531.5 and 530.1 eV. The fitting peaks are due to Si–O bonding, O–H in the hydroxyl groups (such as absorbed H_2O), and Ti–O bonding, which account for 66.2%, 7.6%, and 26.2% relative atomic percentage of O in 1.0%-V/TD, respectively. The shift observed in Ti–O bonding energy might be attributed to the formation of Ti–O–Si bond, resulting from the higher electronegativity of Si in comparison to Ti [39]. The XPS spectrum of the V2p region for 1.0%-V/TD is shown in **Fig. 4d**. The V species exist with a close binding energy value for $V^{5+}2p_{3/2}$ and $V^{4+}2p_{3/2}$. Therefore, the peak fitting at 517.3 eV can be mainly ascribed to $V^{5+}2p_{3/2}$, whereas that at 516.2 eV is assigned to $V^{4+}2p_{3/2}$ [6, 40]. This indicates that V presents in the 1.0%-V/TD hybrids in the form of V^{5+} and V^{4+}, with higher quantity of V^{5+} ions as indicated by the area under the peak in XPS spectrum. According to the literature [36], the presence of V^{4+} ions might be due to the reduction of V^{5+} ions from the starting materials (NH_4VO_3) during the preparation. Due to the similar radii, V^{4+} ions could incorporate in the TiO_2 lattice by substitutionally replacing Ti^{4+} ions and forming Ti–O–V bond.

3.4 UV-visible diffuse reflectance spectra (UV-vis DRS) analysis

It is well known that the photocatalytic activity of a semiconductor catalyst is related to its bandgap structure [25]. The bandgap energy is too large for bulk TiO_2 to absorb visible-light. Therefore, the introduction of V species with different contents is expected to decrease bandgap energy of TiO_2 to some extent. The UV-vis optical absorption spectra obtained by the diffuse reflectance of undoped TiO_2/diatomite and V-TiO_2/diatomite composites are shown in **Fig. 5a**. As we already know, the pure titania shows absorption only in the UV-light region ($\lambda \leq 387$ nm) [41], which is associated with excitation of electrons from O 2p to Ti 3d electronic orbital [42]. Compared with the spectrum of TD, all vanadium doped samples presented the better absorption intensity in UV-light region and an absorption tail in the visible-light region (400–700 nm). Thus, the absorption spectra of V-TiO_2/diatomite hybrids indicate that the trace incorporation of vanadium led to an absorption shift to the visible-light region, which could be ascribed to the formation of isolated impurity energy levels below the bottom of CB [38, 43]. Because of these impurity energy levels within the bandgap, the electrons in the VB can be excited to the impurity energy levels by absorbing visible-light and subsequently transferred to the CB. Using Tauc plot (**Fig. 5b**), i.e. $(F(R)h\nu)^{1/2}$ versus $h\nu$ (mentioned above in **Section 2.3**), the bandgap energy were deduced by extrapolating the linear part of the plot to intersect the photon energy axis. E_g decreases from 3.17 eV (for TD)

to 3.13, 2.95, 3.05 and 3.05 eV with the amount of incorporated V at a V/Ti molar ratio increasing from 0.25%, 0.5%, 1.0% to 1.5% (**Table 1**). Moreover, the narrowing of anatase bandgap is dominantly due to the presence of V^{4+} species in the samples with a relative low content (<1.5% in our case) of vanadium incorporation [31]. Clearly, the higher V-doping (V/Ti=1.0% and 1.5%) causes the bandgap to increase back to 3.05 eV. That is because the dominant presence of vanadium species is V^{5+}, acting as electron acceptor and leading fewer V^{4+} incorporated into TiO_2 lattice [9]. On the contrary, the presence of crystalline V_2O_5 species, having a bandgap of 2 eV [36], on the surface of TiO_2, makes the absorption threshold of 1.0%-V/TD and 1.5%V-TD is still larger than that of undoped sample. The absorption spectra provide thus evidence that V makes a significant influence in the light absorption properties of the composites, with contributions of the co-existence of V^{4+} and V^{5+} by leading a variation of the bandgap and the charge-transfer transition between the *d*-electrons of the dopant and the CB (or VB) of TiO_2 [6, 9]. That is, in the present case, V^{4+} ions present in the substitutional site of Ti^{4+} in TiO_2 lattice are responsible for decreased bandgap energy while V^{5+} ions present on the surface of TiO_2 particle in the form of V_2O_5 species contribute to the efficient e^- and h^+ separation [31]. Due to the lower Fermi level of V_2O_5 species, the photo-generated electrons may immediately transfer to V^{5+} ions leaving back holes on the VB resulting in the effective separation of e^- and h^+ [44].

3.5 Photoluminescence spectra (PL) analysis

The above deduction can be faithfully authenticated by the PL, which is widely used to reflect the fate of photo-generated electron–hole pairs in semiconductor under light illumination. With electron–hole pair recombination after a photocatalyst was irradiated, photons are emitted, resulting in photoluminescence. This behaviour is due to the reverse radiative deactivation from the excited state of the Ti species [45]. **Fig.6** shows the PL spectra of the undoped and vanadium doped TiO_2/diatomite composites with different mole ratios of V/Ti. The broad peak appears at two main regions, 375–425 and 450–500 nm. The former is ascribed to the emission of the bandgap transition, while the latter is emission signal originating from the charge-transfer transition of an oxygen vacancy trapped electron [46-49]. Because the PL emission is the result of the recombination of excited electrons and holes, the lower PL intensity of the doped sample indicates the lower recombination rate. As shown in **Fig.6**, the significant PL quenching of TiO_2 can be observed after doping with vanadium ions.

The decrease in the intensity of PL spectra for the V-doped samples can be explained with the following conclusion. Firstly, some electrons excited by UV-light transfer to the V^{5+} species on the TiO_2 surface from the TiO_2 CB. Secondly, the other electrons excited by visible-light are collected by the newly energy levels (V3d (V^{4+})) generated within the bandgap of TiO_2 [31, 36]) and transfer to V^{5+} species. All these photo-generated electrons then reacted with the oxygen molecules adsorbed on the photocatalyst surface. Therefore, we believe that the decrease in PL intensity is in accordance with the improved electron–hole separation and consequently the enhancement in photocatalytic efficiency of the V-TiO_2/diatomite photocatalyst. In addition, the peak intensity centred at 468 nm decreases first and then increases with an increase in vanadium concentration. This may indicate that excess dopant concentration beyond the optimum value results in the recombination of electron and hole as a consequence of which the photocatalytic efficiency of the catalyst will be decreased.

3.6 Photocatalytic performance

To specify the effect of the doping concentration on the photocatalytic activities, the decomposition of RhB (10 mg/L) under the solar light illumination of V-TiO_2/diatomite in different mole ratios of V/Ti was carried out and compared with undoped TiO_2/diatomite and pure V-TiO_2 particles (shown in **Fig. 7**). The relative concentrations of RhB were fitted by the apparent first-order rate equation as follows:

$$-\ln(\frac{C}{C_o}) = kt \qquad (1)$$

where C is the RhB concentration at time t, and k is the apparent reaction rate constant. The results are listed in **Table 2**. The table shows that the order of photocatalytic activity of the as-prepared samples was 0.5%-V/TD > 1.0%-V/TD > 1.5%-V/TD > 0.25%-V/TD > TD under solar light illumination. The photocatalytic activity was enhanced and then decreased with an increase in the doping content of vanadium. Clearly, the activity results indicate that V doped TiO_2/diatomite photocatalyst showed higher activity than undoped TiO_2/diatomite. This improvement is probably due to the increase in the visible-light absorption on the consequence of decrease in the bandgap energy with vanadium doping. In addition to lower bandgap energy there are several other factors that may have contributed towards higher photocatalytic activity, including the declined electron-hole recombination rate. As confirmed

above, the V dopants in our work present in the form of V^{4+} and V^{5+} ions. The V^{4+} substitutionally replaces Ti^{4+} ions in the TiO_2 to form isolated impurity levels around 0.8 to 1.0 eV below the CB of TiO_2 [38]. On the other hand, V^{5+} species trap the photo-generated electrons and leave back holes in VB resulting in the efficient separation of e^- and h^+, due to the lower Fermi level of V_2O_5 species [36]. These photo-generated electrons may react with the oxygen molecules adsorbed on the surface of TiO_2 to produce the oxidant superoxide radicals $\cdot O_2^-$. As we can see in PL spectra of undoped and V doped TiO_2/diatomite samples (**Fig.6**), the vanadium doping inhibits the recombination rate effectively, resulting in the improvement of the photocatalytic efficiency. The photocatalytic activity of 1.5%-V/TD declined significantly due to the overmuch doping concentration, which leads to the fast recombination of hole and electron pairs. The apparent reaction constants of 0.5%-V/TD, 1.0%-V/TD and 1.5%-V/TD with efficient improvement towards RhB were 7.19, 7.17, and 5.13 times higher than that of undoped sample, respectively.

In order to highlight the function of diatomite support, we also prepared a series of pure V-TiO_2 samples with the same doping concentration. During the photocatalytic test we used the same amount of pure V-TiO_2 and V-TiO_2/diatomite samples, as shown in **Fig. 7a** and **b**. The sample without diatomite (1.0%-V/T) only has the degradation efficiency of 53.74% for RhB after illumination for 5 hrs. Comparatively speaking, the sample supported by diatomite (1.0%-V/TD) displays the degradation efficiency of 88.42% for RhB under the same solar light illumination. We speculate the reasonable explanation is the introduction of diatomite may make the photocatalytic TiO_2 nanoparticle with small size and well dispersion in suspension system. That is, this form facilitates the e^- and h^+ transport to the surface for the following reaction and enlarges the active surface area for reactants and light. Furthermore, the weight ratio of TiO_2 in this hybrid is only 10%. In the view point of practical applications, such a low TiO_2 component and doping content meet the requirements for building low-cost photocatalysts that need impressive visible-light activity.

The reusability of the 1.0%-V/TD sample was also investigated. As shown in **Fig. 7c**, the composite shows good reusability. The photocatalytic activity remains well after four reaction cycles. Additionally, the reused hybrid catalysts still exhibited certain adsorption towards RhB and reached equilibrium within 60 min. Compared with the performance in the first run, the fourth run presents slightly lower activity, which may be ascribed to

intermediate poison to composite surface. The intermediates from RhB degradation could be adsorbed on catalyst surface, making low light absorption and electron transfer for photocatalysis [50]. Most importantly, this micro-size hybrid catalyst could settle down naturally within 30 min, while to separate Degussa P25 or other nano-size catalysts centrifugation is necessary.

4. Conclusion

The photocatalytic activity of V doped TiO_2/diatomite composite, synthesized by sol–gel method, for the degradation of RhB under solar light illumination is significantly improved as compared to the undoped sample and unsupported sample. On the basis of physiochemical analysis, V^{4+} and V^{5+} species were co-exist in our case. V^{4+} ions presented in the substitutional site of Ti^{4+} in TiO_2 lattice are responsible for increased visible-light absorption. In the meantime, V^{5+} species presented on the surface of TiO_2 particles in the form of V_2O_5 are responsible for the efficient e^-–h^+ separation and enhanced charge-transfer transition towards oxygen molecules adsorbed on the surface of TiO_2 for producing $\cdot O_2^-$. The photodegradation rate of 0.5%-V/TD was approximately 7.19 times higher than that of the undoped sample. Overall, this work provides a strategy for the further enhancement of photoactivity of the TiO_2/mineral composite catalyst, which may contribute to the deep environmental remediation using cost-effective photocatalyst. An interesting use of this vanadium doped TiO_2/diatomite composites in photocatalytic applications is as filler of coating to purify the indoor volatile organic compounds.

Acknowledgement

The authors gratefully acknowledge the financial support provided by National Technology R&D Program in the 12th five years plan of China (2011BAB03B07). The first author thanks the Cultivation Project of Top Creative Talents Ph D student from China University of Mining &Technology (Beijing) for financial support. The first author also thanks the China Scholarship Council (CSC) for financial support. And also the first author appreciates Professor Ian R. Gentle's suggestion and support, which make the first author be able to do experiments in School of Chemistry and Molecular Biosciences, The University of Queensland.

References

[1] U.G. Akpan, B.H. Hameed, Parameters affecting the photocatalytic degradation of dyes using TiO_2-based photocatalysts: A review, J. Hazard. Mater. 170 (2009) 520-529.

[2] X. Wang, L. Sø, R. Su, S. Wendt, P. Hald, A. Mamakhel, C. Yang, Y. Huang, B.B. Iversen, F. Besenbacher, The influence of crystallite size and crystallinity of anatase nanoparticles on the photo-degradation of phenol, J. Catal. 310 (2014) 100-108.

[3] M. Pelaez, N.T. Nolan, S.C. Pillai, M.K. Seery, P. Falaras, A.G. Kontos, P.S. Dunlop, J.W. Hamilton, J.A. Byrne, K. O'Shea, A review on the visible light active titanium dioxide photocatalysts for environmental applications, Appl. Catal., B 125 (2012) 331-349.

[4] N. Murakami, T. Chiyoya, T. Tsubota, T. Ohno, Switching redox site of photocatalytic reaction on titanium (IV) oxide particles modified with transition-metal ion controlled by irradiation wavelength, Appl. Catal., A 348 (2008) 148-152.

[5] M. Anpo, Preparation, characterization, and reactivities of highly functional titanium oxide-based photocatalysts able to pperate under UV-visible light irradiation: Approaches in realizing high efficiency in the use of visible light, Bull. Chem. Soc. Jpn. 77 (2004) 1427-1442.

[6] X. Yang, F. Ma, K. Li, Y. Guo, J. Hu, W. Li, M. Huo, Y. Guo, Mixed phase titania nanocomposite codoped with metallic silver and vanadium oxide: New efficient photocatalyst for dye degradation, J. Hazard. Mater. 175 (2010) 429-438.

[7] J. Zhou, M. Takeuchi, A.K. Ray, M. Anpo, X.S. Zhao, Enhancement of photocatalytic activity of P25 TiO_2 by vanadium-ion implantation under visible light irradiation, J. Colloid Interface Sci. 311 (2007) 497-501.

[8] M. Bettinelli, V. Dallacasa, D. Falcomer, P. Fornasiero, V. Gombac, T. Montini, L. Romanò, A. Speghini, Photocatalytic activity of TiO_2 doped with boron and vanadium, J. Hazard. Mater. 146 (2007) 529-534.

[9] A. Kubacka, A. Fuerte, A. Martínez-Arias, M. Fernández-García, Nanosized Ti–V mixed oxides: Effect of doping level in the photo-catalytic degradation of toluene using sunlight-type excitation, Appl. Catal., B 74 (2007) 26-33.

[10] M.D. Hernández-Alonso, F. Fresno, S. Suárez, J.M. Coronado, Development of alternative photocatalysts to TiO_2: Challenges and opportunities, Energy Environ. Sci. 2 (2009) 1231-1257.

[11] L. Andronic, D. Perniu, A. Duta, Synergistic effect between TiO_2 sol–gel and Degussa P25 in dye photodegradation, J. Sol-Gel Sci. Technol. 66 (2013) 472-480.

[12] Y.Y. Guo, X.P. Pu, D.F. Zhang, G.Q. Ding, X. Shao, J. Ma, Combustion synthesis of graphene oxide–TiO_2 hybrid materials for photodegradation of methyl orange, Carbon 50 (2012) 4093-101.

[13] P. Gao, A.R. Li, D.D. Sun, W.J. Ng, Effects of various TiO_2 nanostructures and graphene oxide on photocatalytic activity of TiO_2, J. Hazard. Mater. 279 (2014) 96-104.

[14] X.P. Pu, D.F. Zhang, Y.Y. Guo, X. Shao, G.Q. Ding, S.S. Li, SH.P. Zhao, One-pot microwave-assisted combustion synthesis of graphene oxide–TiO_2 hybrids for photodegradation of methyl orange, J. Alloys Compd., 2013, 551, 382-388. .

[15] S.W. Lee, J. Drwiega, C.Y. Wu, D. Mazyck, W.M. Sigmund, Anatase TiO_2 nanoparticle coating on barium ferrite using titanium bis-ammonium lactato dihydroxide and its use as a magnetic photocatalyst. Chem Mater, 16 (2004) 1160-1164. .

[16] P. Gao, J. Liu, S. Lee, T. Zhang, D.D. Sun, High quality graphene oxide–CdS–Pt nanocomposites for efficient photocatalytic hydrogen evolution, J. Mater. Chem. 22 (2012) 2292–2298.

[17] D. Kibanova, J. Cervini-Silva, H. Destaillats, Efficiency of clay−TiO_2 nanocomposites on the photocatalytic elimination of a model hydrophobic air pollutant, Environ. Sci. Technol. 43 (2009) 1500-1506.

[18] D. Kibanova, M. Sleiman, J. Cervini-Silva, H. Destaillats, Adsorption and photocatalytic oxidation of formaldehyde on a clay-TiO_2 composite, J. Hazard. Mater. 211–212 (2012) 233-239.

[19] H. Destaillats, D. Kibanova, M. Trejo, H. Destaillats, J. Cervini-Silva, Synthesis of hectorite-TiO_2 and kaolinite-TiO_2 nanocomposites with photocatalytic activity for the degradation of model air pollutants, Appl. Clay Sci. 42 (2009).

[20] B. Wang, G. Zhang, Z. Sun, S. Zheng, Synthesis of natural porous minerals supported TiO_2 nanoparticles and their photocatalytic performance towards Rhodamine B degradation, Powder Technol. 262 (2014) 1-8.

[21] Z. Sun, C. Bai, S. Zheng, X. Yang, R.L. Frost, A comparative study of different porous amorphous silica minerals supported TiO_2 catalysts, Appl. Catal., A 458 (2013) 103-110.

[22] X. He, A. Tang, H. Yang, J. Ouyang, Synthesis and catalytic activity of doped TiO_2-palygorskite composites, Appl. Clay Sci. 53 (2011) 80-84.

[23] C. Huo, H. Yang, Preparation and enhanced photocatalytic activity of Pd–CuO/palygorskite nanocomposites, Appl. Clay Sci. 74 (2013) 87-94.

[24] Z. Sun, X. Yang, G. Zhang, S. Zheng, R.L. Frost, A novel method for purification of low grade diatomite powders in centrifugal fields, Int. J. Miner.l Process. 125 (2013) 18-26.

[25] M. Nasir, Z. Xi, M. Xing, J. Zhang, F. Chen, B. Tian, S. Bagwasi, Study of synergistic effect of Ce- and S-codoping on the enhancement of visible-light photocatalytic activity of TiO_2, J. Phys. Chem. C 117 (2013) 9520-9528.

[26] V. Nadtochenko, N. Denisov, A. Gorenberg, Y. Kozlov, P. Chubukov, J.A. Rengifo, C. Pulgarin, J. Kiwi, Correlations for photocatalytic activity and spectral features of the absorption band edge of TiO_2 modified by thiourea, Appl. Catal., B 91 (2009) 460-469.

[27] Z. Zhang, C. Shao, L. Zhang, X. Li, Y. Liu, Electrospun nanofibers of V-doped TiO_2 with high photocatalytic activity, J. Colloid Interface Sci. 351 (2010) 57-62.

[28] A. Vittadini, M. Casarin, M. Sambi, A. Selloni, First-principles studies of vanadia−titania catalysts: Beyond the monolayer, J. Phys. Chem. B 109 (2005) 21766-21771.

[29] D.E. Gu, B.C. Yang, Y.D. Hu, V and N co-doped nanocrystal anatase TiO_2 photocatalysts with enhanced photocatalytic activity under visible light irradiation, Cataly. Commun. 9 (2008) 1472-1476.

[30] L. Li, C.Y. Liu, Y. Liu, Study on activities of vanadium (IV/V) doped TiO_2 (R) nanorods induced by UV and visible light, Mater. Chem. Phys. 113 (2009) 551-557.

[31] J. Liu, R. Han, Y. Zhao, H. Wang, W. Lu, T. Yu, Y. Zhang, Enhanced photoactivity of V−N codoped TiO_2 derived from a two-step hydrothermal procedure for the degradation of PCP−Na under visible light irradiation, J. Phys. Chem. C 115 (2011) 4507-4515.

[32] D. Bersani, P.P. Lottici, X.-Z. Ding, Phonon confinement effects in the Raman scattering by TiO_2 nanocrystals, Appl. Phys. Lett. 72 (1998) 73-75.

[33] S. Sahoo, A.K. Arora, V. Sridharan, Raman line shapes of optical phonons of different symmetries in anatase TiO_2 nanocrystals, J. Phys. Chem. C 113 (2009) 16927-16933.

[34] B. Choudhury, B. Borah, A. Choudhury, Ce–Nd codoping effect on the structural and optical properties of TiO_2 nanoparticles, Mater. Sci. Eng., B 178 (2013) 239-247.

[35] H. Lin, Y. Chou, C. Cheng, Y. Chen, Giant enhancement of band edge emission based on ZnO/TiO_2 nanocomposites, Opt. Express, 15 (2007) 13832-13837.

[36] R. Jaiswal, N. Patel, D.C. Kothari, A. Miotello, Improved visible light photocatalytic activity of TiO_2 co-doped with vanadium and nitrogen, Appl. Catal., B 126 (2012) 47-54.

[37] R. Sanjinés, H. Tang, H. Berger, F. Gozzo, G. Margaritondo, F. Lévy, Electronic structure of anatase TiO_2 oxide, J. Appl. Phys. 75 (1994) 2945-2951.

[38] R. Dholam, N. Patel, A. Miotello, Efficient H_2 production by water-splitting using indium–tin-oxide/V-doped TiO_2 multilayer thin film photocatalyst, Int. J. Hydrogen Energy 36 (2011) 6519-6528.

[39] Y.L. Lin, T.J. Wang, Y. Jin, Surface characteristics of hydrous silica-coated TiO_2 particles, Powder Technol. 123 (2002) 194-198.

[40] B.M. Reddy, P.M. Sreekanth, E.P. Reddy, Y. Yamada, Q. Xu, H. Sakurai, T. Kobayashi, Surface characterization of La_2O_3−TiO_2 and V_2O_5/La_2O_3−TiO_2 catalysts, J. Phys. Chem. B 106 (2002) 5695-5700.

[41] D. Mitoraj, H. Kisch, The nature of nitrogen-modified titanium dioxide photocatalysts active in visible light, Angew. Chem. Int. Ed. 47 (2008) 9975-9978.

[42] W. Xue, G. Zhang, X. Xu, X. Yang, C. Liu, Y. Xu, Preparation of titania nanotubes doped with cerium and their photocatalytic activity for glyphosate, Chem. Eng. J. 167 (2011) 397-402.

[43] X. Ma, L. Miao, S. Bie, J. Jiang, Synergistic effect of V/N-codoped anatase photocatalysts, Solid State Commun. 150 (2010) 689-692.

[44] Y. Wang, Y.R. Su, L. Qiao, L.X. Liu, Q. Su, C.Q. Zhu, X.Q. Liu, Synthesis of one-dimensional TiO_2/V_2O_5 branched heterostructures and their visible light photocatalytic activity towards Rhodamine B, Nanotechnology 22 (2011) 225702–225709.
[45] Y.J. Xu, Y. Zhuang, X. Fu, New insight for enhanced photocatalytic activity of TiO_2 by doping carbon nanotubes: A aase study on degradation of benzene and methyl orange, J. Phys. Chem. C 114 (2010) 2669-2676.
[46] F.B. Li, X.Z. Li, The enhancement of photodegradation efficiency using Pt–TiO_2 catalyst, Chemosphere 48 (2002) 1103-1111.
[47] D. Li, H. Haneda, S. Hishita, N. Ohashi, Visible-light-driven N−F−codoped TiO_2 photocatalysts. 2. Optical characterization, photocatalysis, and potential application to air purification, Chem. Mater. 17 (2005) 2596-2602.
[48] J. Zhang, Y. Hu, M. Matsuoka, H. Yamashita, M. Minagawa, H. Hidaka, M. Anpo, Relationship between the local structures of titanium oxide photocatalysts and their reactivities in the decomposition of NO, J. Phys. Chem. B 105 (2001) 8395-8398.
[49] H. Khan, D. Berk, Sol–gel synthesized vanadium doped TiO_2 photocatalyst: Physicochemical properties and visible light photocatalytic studies, J. Sol-Gel Sci. Technol. 68 (2013) 180-192.
[50] S. Liu, H. Sun, A. Suvorova, S. Wang, One-pot hydrothermal synthesis of ZnO-reduced graphene oxide composites using Zn powders for enhanced photocatalysis, Chem. Eng. J. 229 (2013) 533-539.

Figure captions:

Figure 1 XRD patterns for the diatomite, TiO_2/diatomite and V-TiO_2/diatomite composites: (a) DE, (b) TD, (c) 0.25%-V/TD, (d) 0.5%-V/TD, (e) 1.0%-V/TD and (f) 1.5%-V/TD.

Figure 2 Raman spectra for the undoped and vanadium doped TiO_2/diatomite composites.

Figure 3 TEM images of (a) purified diatomite (DE), (b-c) undoped TiO_2/diatomite, and (d) 1.0%-V/TD sample. ***Inset*** shows the corresponding EDX result.

Figure 4 (A) XPS survey spectra of (a) TD, (b) 0.25%-V/TD, (c) 0.5%-V/TD, (d) 1.0%-V/TD and (e) 1.5%-V/TD; (B) Ti2p levels of (a) TD, (b) 0.25%-V/TD, (c) 0.5%-V/TD, (d) 1.0%-V/TD and (e) 1.5%-V/TD; (C) and (D) are the O1s and V2p levels for the sample 1.0%-V/TD.

Figure 5 (a) UV-vis diffuse reflectance spectra (DRS) of the undoped and V-doped TiO_2/diatomite composites and (b) the plot of transformed Kubelka–Munk function versus the energy of light.

Figure 6 Photoluminescence spectra (λ_{ex}=320 nm) of the undoped and vanadium doped TiO_2/diatomite composites.

Figure 7 Photodegradation of RhB over pure TiO_2 and undoped and vanadium doped TiO_2/diatomite composites (a), first-order kinetics plots (b), and reusability test of 1.0%-V/TD (c) under solar light.

Table 1

Physiochemical properties of undoped and vanadium doped TiO_2/diatomite composites

Sample	Crystalline size (nm)	Bandgap energy (eV)
TD	16.69	3.17
0.25%-V/TD	13.21	3.13
0.5%-V/TD	16.49	2.95
1.0%-V/TD	20.88	3.05
1.5%-V/TD	22.27	3.05

Table 2

Photocatalytic activity of undoped and vanadium doped TiO_2/diatomite composites

Sample	k ($10^{-3}min^{-1}$)	R^2
TD	1.19	0.99611
0.25%-V/TD	1.66	0.99680
0.5%-V/TD	8.56	0.99742
1.0%-V/TD	8.53	0.99926
1.5%-V/TD	6.10	0.99669

Fig.1

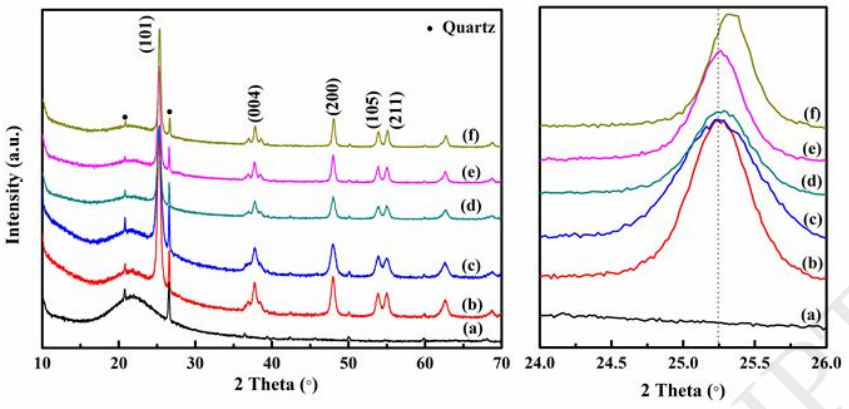

Fig.1

Fig.2

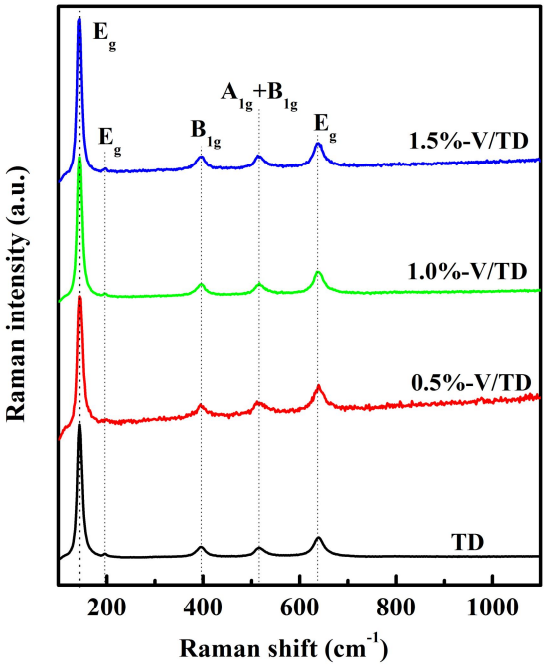

Fig2 .

Fig.3.

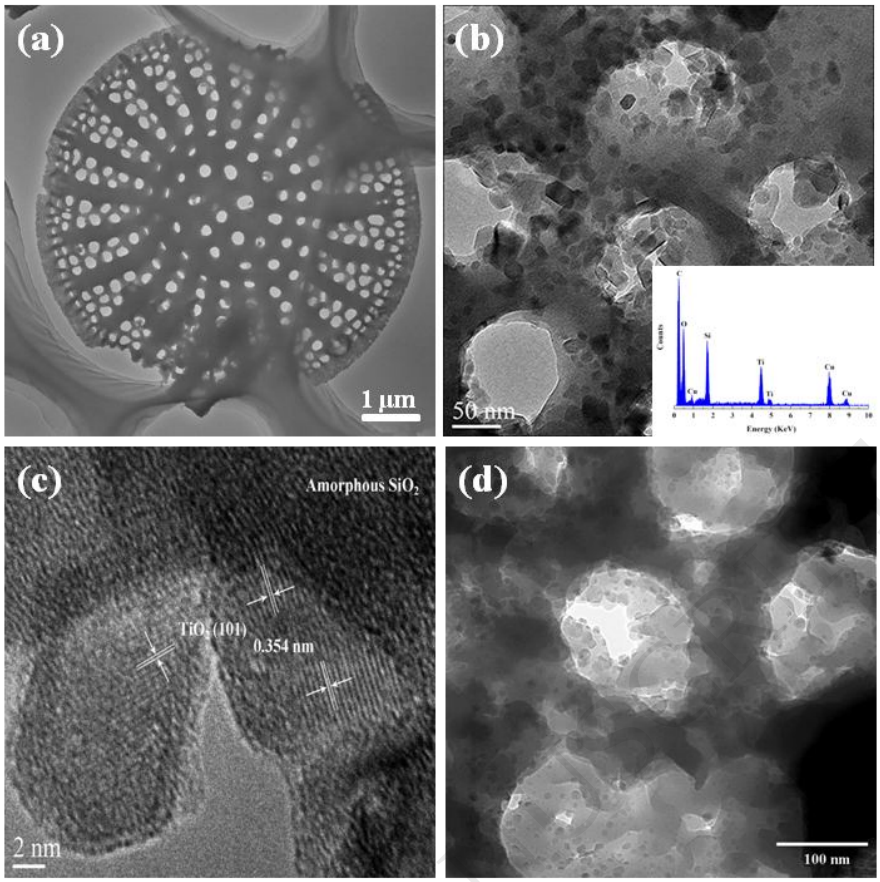

Fig.4A

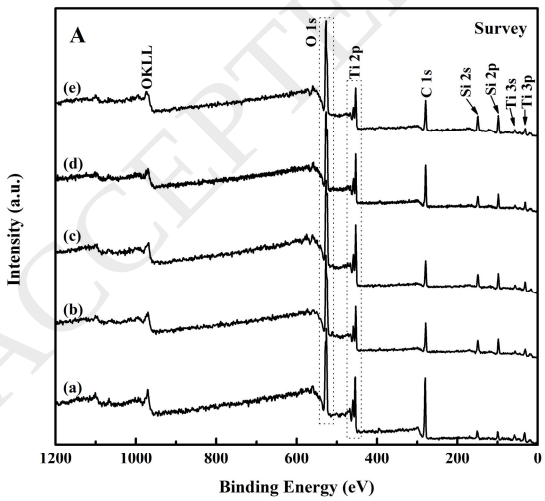

Fig.4a

Fig.4B

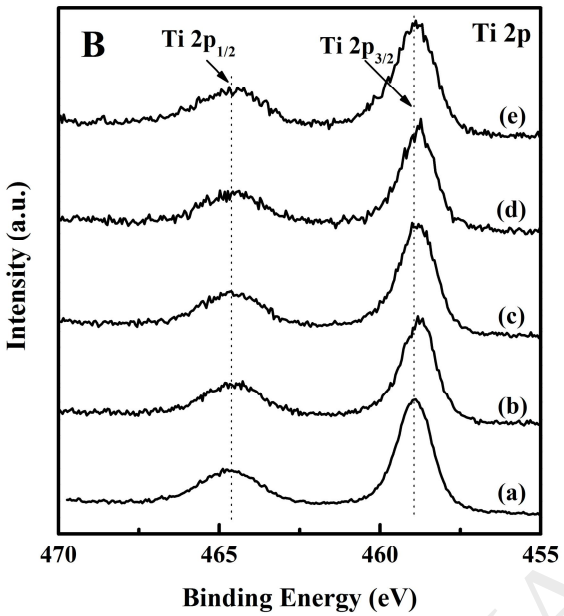

Fig.4b.

Fig.4C

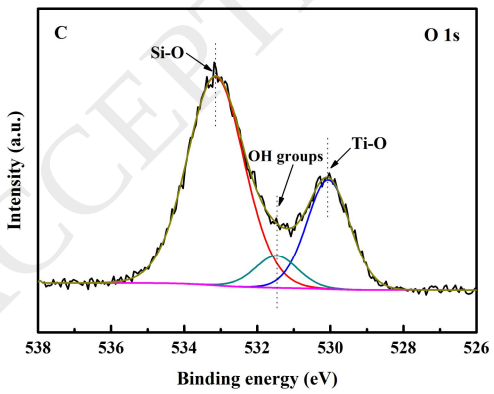

Fig.4c.

Fig.4D

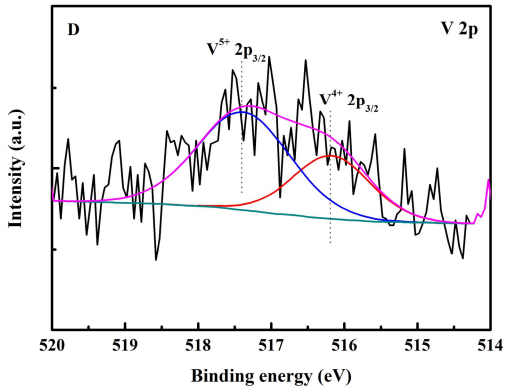

Fig.4d.

Fig.5A

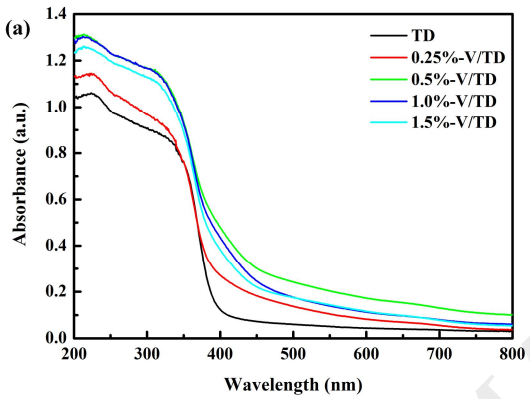

Fig.5a.

Fig.5B

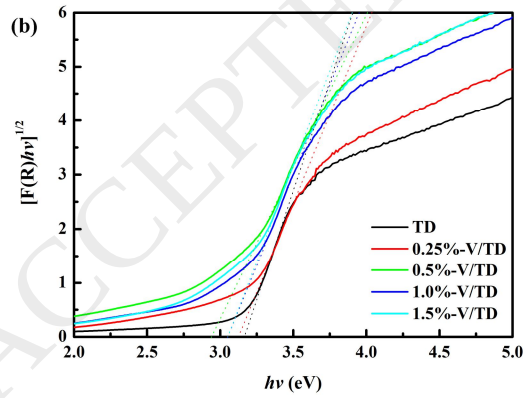

Fig.5b.

Fig.6

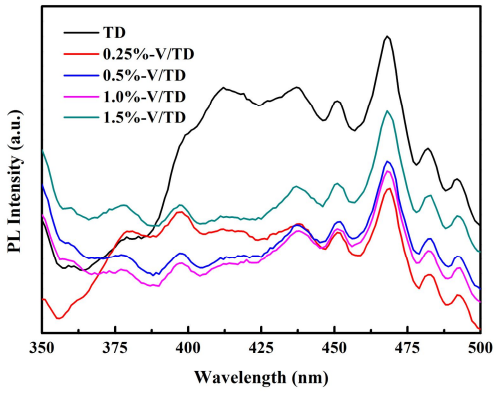

Fig.6.

Fig.7c

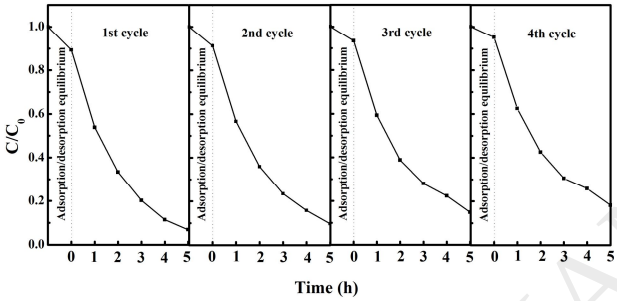

Fig.7c.

Fig.7a

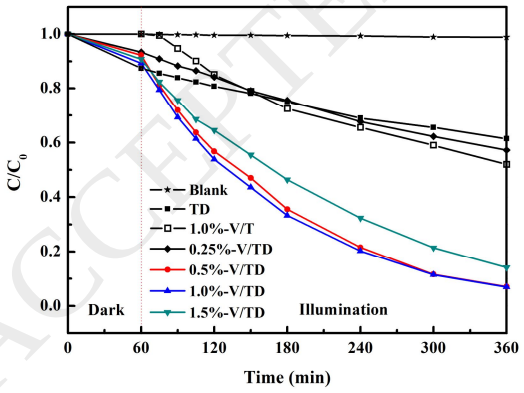

Fig.7a.

Fig.7b

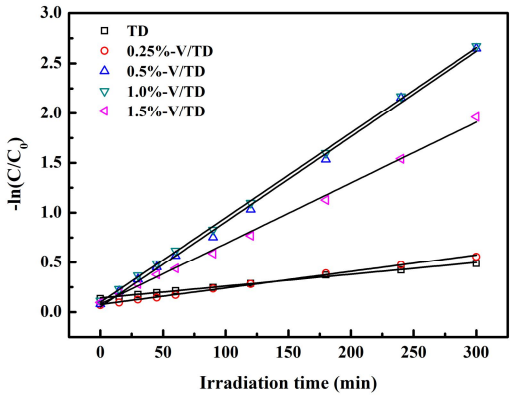

Fig.7b